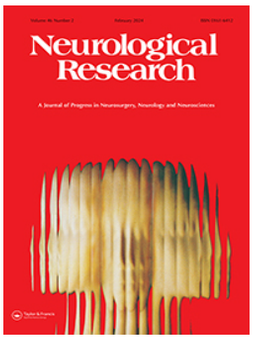

Taylor & Francis
Taylor & Francis Group

Neurological Research

A Journal of Progress in Neurosurgery, Neurology and Neurosciences

ISSN: 0161-6412 (Print) 1743-1328 (Online) Journal homepage: www.tandfonline.com/journals/yner20

Protective effect of melatonin on blood-brain barrier damage caused by Endotoxemia

Kubra Tugce Kalkan, Mukaddes Esrefoglu, Sule Terzioglu-Usak & Arzu Yay

To cite this article: Kubra Tugce Kalkan, Mukaddes Esrefoglu, Sule Terzioglu-Usak & Arzu Yay (2024) Protective effect of melatonin on blood-brain barrier damage caused by Endotoxemia, Neurological Research, 46:2, 195-206, DOI: 10.1080/01616412.2023.2265244

To link to this article: https://doi.org/10.1080/01616412.2023.2265244

NEUROLOGICAL RESEARCH
2024, VOL. 46, NO. 2, 195–206
https://doi.org/10.1080/01616412.2023.2265244

Taylor & Francis
Taylor & Francis Group

Protective effect of melatonin on blood-brain barrier damage caused by Endotoxemia

Kubra Tugce Kalkan [a,b], Mukaddes Esrefoglu [c], Sule Terzioglu-Usak [d] and Arzu Yay [b,e]

[a]Department of Histology and Embryology, Faculty of Medicine, Kırşehir Ahi Evran University, Kırşehir, Turkey; [b]Department of Histology and Embryology, Faculty of Medicine, Erciyes University, Kayseri, Turkey; [c]Department of Histology and Embryology, Faculty of Medicine, Bezmialem Vakif University, Istanbul, Turkey; [d]Erfe Group Company, Istanbul, Turkey; [e]Genome and Stem Cell Center (GENKOK), Erciyes University, Kayseri, Turkey

ABSTRACT

Objective: Endotoxins, products of Gram-negative bacteria, are the primary cause of blood-brain barrier (BBB) damage. In the present study, we aimed to investigate the possible neuroprotection mechanisms of melatonin on BBB damage induced by endotoxemia.

Methods: Adult, female Sprague-Dawley rats ($n = 42$) were separated into four random groups as a control group and three treatment groups. Lipopolysaccharide (7,5 mg/kg/day) was administrated for a single dose to generate a 24-hour sepsis model on rats. Melatonin (10 mg/kg/day) was treated a week before sepsis. Afterward, the dissected brain tissues were examined by histopathological, biochemical, and molecular analyses.

Results: LPS caused weight loss in the groups. As a result, degenerated neurons with cytoplasmic vacuoles and irregular pyknotic nuclei, pale stained necrotic neurons, and vascular congestion were observed in LPS-exposed rats. However, MEL decreased the number of degenerated neurons in treated groups. MEL treatment increased ZO1 and Occludin immunoreactivity while decreasing TLR4 in brain tissues. MEL effect on protein expression was recorded for ZO1 increase and TLR4 decrease in brain tissue compared to LPS groups. MEL also decreased MDA levels in brain tissue.

Conclusions: MEL recovered the degenerative damage of sepsis by contributing to blood-brain barrier integrity, and by decreasing inflammation, thus the neuroprotective effects of MEL might provide an experimental basis for clinical applications.

ARTICLE HISTORY
Received 31 March 2023
Accepted 24 September 2023

KEYWORDS
Endotoxemia; lipopolysaccharide; melatonin; brain; rat

Introduction

Endotoxemia is a systemic inflammatory response syndrome with a high incidence and mortality rates worldwide [1]. Lipopolysaccharide (LPS) is a major constituent of gram-negative bacterial endotoxin, which causes multiple organ damage in endotoxemia [2]. The central nervous system (CNS) is known to be most affected by sepsis caused by LPS administration [3–6].

The blood-brain barrier (BBB) is mainly composed of brain capillary endothelial cells, basement membrane, pericytes, and astrocyte end feet [7,8] and protects CNS homeostasis [9,10]. The junctional complexes between brain capillary endothelial cells include adherens junctions and tight junctions [11]. Occludin and claudins are a member of tight junctions linked to several cytoplasmic scaffolding and regulatory proteins ZO-1, ZO-2, ZO-3, and cingulin [8,11]. An inflammation may induce a BBB disruption in the functions of those tight junctions [12,13]. For instance, it has been discovered that changes in the permeability of BBB are connected to sepsis, meningitis, encephalitis, and other local and systemic infections. Several neurological illnesses have a direct association with damage in BBB. Multiple sclerosis, Alzheimer's, Parkinson's, Huntington's, and other neurodegenerative illnesses are all brought on by the neuroinflammation that results from this process [14,15–18].

Toll-like receptor (TLR) proteins are encoded by Toll genes. TLR 1, 2, 4, 5, 6, and 10 usually settle on the cell surface and recognize molecules specific to pathogens. On the other hand, TLR 3, 7, 8, and 9 settle inside the intracellular organelles [19,20]. TLR signaling mechanism is induced by the production of molecules such as proinflammatory cytokines and nitric oxide, and thus immune system cells in the early stage of infection are activated for the elimination of microorganisms. LPS as an outer membrane component of gram-negative bacteria is detected by the immune system through toll-like receptor-4 (TLR-4) [21].

Melatonin (MEL) is a dark hormone synthesized and released from the pineal gland. MEL shows its effects through melatonin receptors in the cell membrane and by combining with G proteins, a secondary carrier [22]. Although MEL has chronobiological

CONTACT Arzu Yay arzu.yay38@gmail.com Department of Histology and Embryology, Medicine Faculty, University of Erciyes , Genome and Stem Cell Center (GENKOK), Erciyes University, Kayseri TR-38039, Turkey

functions, it also has antioxidant, anti-inflammatory, anticancer, antiaging, and immune modulatory effects. This hormone has a small molecule size and high lipophilic properties. Thus, it passes through biological membranes and is distributed to all tissues and fluids [23]. The night hormone can easily pass through BBB and comfortably shows its effect on CNS [24].

In this study, it was aimed to investigate possible neuroprotection mechanisms of melatonin on BBB damage induced by endotoxemia.

Materials and methods

Animals

Adult, female 6-month-old Sprague-Dawley rats (n = 42) (weighing 150–250 g) were housed with ad libitum access to water and a standard diet under stress-free, standard conditions (21°C;12 light/12 dark cycles). The Guide for the Care and Use of Laboratory Animals adopted by the National Institutes of Health (U.S.A.) and the Declaration of Helsinki were followed during experiments. The experimental protocol of this study was approved by Bezmialem Vakıf University Local Ethics Committee for Animal Experiments (2018/131).

Study design

The rats were randomly divided into four groups: control (n = 8), lipopolysaccharide (LPS; n = 13), lipopolysaccharide+melatonin (LPS+MEL; n = 13), and melatonin (MEL; n = 8). Only one dose of LPS (7,5 mg/kg/day) was administered (Escherichia coli-serotype O111:B4; Sigma-Aldrich Co., St. Louis, MO, U.S.A.), and a 24-hour sepsis model was created. MEL (M 5250; Sigma, St Louis, MO, U.S.A.) treatment (10 mg/kg/day) was started one week before LPS administration. MEL was dissolved in pure ethanol and diluted with physiological saline to a concentration of 1% and applied. The control group was injected with 0.9% NaCl saline solution. At the end of the experiment, the rats were decapitated under anesthesia, and their brain tissues were dissected. The right lobes of the brain were used in histological examinations, while the left lobes were stored at −80°C for biochemical analyses.

Histopathological analyses

10% neutral buffered formaldehyde fixed brain tissues were dehydrated by passing through increasing concentrations of alcohol, cleared by passing through xylol, and finally embedded in paraffin blocks. The sections approximately 5-µm in thickness were stained with hematoxylin-eosin (H&E), Masson's trichrome, and cresyl violet acetate. All samples were examined with a light microscope (Olympus BX51, Tokyo, Japan) and then photographed.

Immunohistochemistry

Immunohistochemical stainings of ZO-1, Occludin, and TLR-4 expressions were carried out by using the streptavidin-biotin-peroxidase technique. Briefly, 5-µm of brain sections were deparaffinized in xylene and rehydrated through a graded ethanol series. Following that, they were rinsed in deionized water. The sections were washed with phosphate-buffered saline (PBS), and then treated with hydrogen peroxide of 3% for 5 min to avoid endogenous peroxidase activity. After washing with PBS again, they were placed in 10% citrate buffer (pH 6.0) in a microwave oven at 95°C for 5 min for antigen recovery and kept in the same buffer solution at room temperature for 20 min. The procedure was followed by using an immunohistochemistry staining kit (Invitrogen, Histostain ® -plus 3rd Gen IHC Detection Kit, California, U.S.A.). The sections were incubated with ZO-1 primary antibody (1:500) (Millipore MABT 339, Massachusetts, U.S.A.), Occludin primary antibody (1:50) (Thermo Fischer 71–1500, Massachusetts, U.S.A.), and TLR-4 primary antibody (1:50) (Santa Cruz Biotechnology sc -293,072, Oregon, U.S.A.) overnight at 4°C. Then, the sections were incubated with biotinylated secondary antibodies. After washing, the streptavidin-peroxidase complex was applied and 3,3'-p-diaminobenzidine tetrahydrochloride chromogen was used. The sections were counterstained with Gill's hematoxylin to increase nuclear staining. Images were captured from 10 independent areas for each section of the cerebral cortex by using a digital camera (DP71) attached to a light microscope (Olympus BX51, Tokyo, Japan). Immunoreactivity densities of ZO-1, Occludin, and TLR-4 were calculated using the Image J software program (NIH; Washington, U.S.A.).

Enzyme-linked immunosorbent assay (ELISA)

Frozen brain tissues were complemented with PBS (0.01 M, pH: 7.4), homogenized, and centrifuged at 10,000 rpm for 10 min at 4°C. The collected supernatants were aliquoted for the ELISA procedure. The antioxidant levels of tissues were determined by superoxide dismutase (SOD) (Sunred Biological Technology, 201-11-0169, Shanghai, China), catalase (CAT) (Sunred Biological Technology, 201-11-5106, Shanghai, China), glutathione peroxidase (GSH-Px) (Sunred Biological Technology, 201-11-5104, Shanghai, China) measurements as well as the lipid peroxidation level were examined by malondialdehyde (MDA) (Sunred Biological Technology, 201-11-0157, Shanghai, China) measurement. In addition, the inflammation was determined by

Transformative Growth Factor-Beta (TGF-β) (Sunred Biological Technology 201-11-0779, Shanghai, China), Tumor Necrosis Factor-Alpha (TNF-α) (Sunred Biological Technology 201-11-0765, Shanghai, China), Interleukin 1-beta (IL-1β) (Bioassay Technology Laboratory, E0119Ra, Shanghai, China), Nuclear Factor-Kappa Beta (NF-κB) (Technology Laboratory, E0287Ra, Shanghai, China) levels. All ELISA kits were performed according to the manufacturer's procedures stated in the commercial kits.

Western blotting

Frozen brain tissues were homogenized in RIPA lysis buffer (Santa Cruz Biotechnology, sc -24,948, Santa Cruz, CA, U.S.A.), and centrifuged at 15,000 rpm for 15 min at 4°C. The collected supernatants were used for sodium dodecyl sulfate-polyacrylamide gel electrophoresis (SDS-PAGE). The concentrations of protein which were determined with Pierce BCA Protein Assay Kit (Thermo Fisher Scientific, Waltham) by Multiskan™ GO Microplate Spectrophotometer, were diluted in sample buffer and boiled. Equal amounts of protein were loaded on an SDS – PAGE gel (Mini-Protean ® TGX Precast Gels, 456–1035, U.S.A.) and run using electrophoresis and then transferred to a PVDF membrane using a semi-dry blotting system (Trans-Blot Turbo system, Bio-Rad Laboratories, U.S.A.), blocked in skimmed milk solution (5% milk powder in 0.1% Tween 20/0.1 M Tris-buffered saline (TBST)) for 1 h. Then, the membranes were incubated with primary antibodies against ZO-1 (1:1000; Millipore MABT 339, Massachusetts, U.S.A.), Occludin (1:1000; Thermo Fischer, 71–1500, Massachusetts, U.S.A.), TLR-4 (1:1000; Santa Cruz Biotechnology, sc -293,072, Oregon, U.S.A.) overnight at 4°C. The membranes were also incubated with mouse anti-β-actin (1:3000, 4970, Cell Signaling Technologies, U.S.A.) as a loading control. After the removal of excessive primary antibodies on the next day, the membranes were then incubated with HRP-conjugated secondary antibodies (anti-rabbit 1:5000, Advansta; anti-mouse 1:5000, Advansta, California, U.S.A.) at room temperature for 1 h. The signal detection was achieved by treating the membranes with ECL (Western Bright Sirius K-12043-D10, Advansta, California, U.S.A.), and by visualizing through a gel imaging system (Fusion F×7Vilber Lourmat, Marne-la-Vallee, France). Experiments were repeated independently three times. Immunoreactive protein bands were quantified densitometrically using the ImageJ analysis system (NIH; Washington, U.S.A.).

Statistical analysis

All statistical analyses were performed using the 'Graph Pad Prism Version 8.1' statistical software program. The Shapiro-Wilk test was used to determine the distribution of data. One-way analysis of variance (ANOVA) and Kruskal Wallis tests were used for more than two intergroup comparisons. Post-hoc comparisons of variables were found to be significant as a result of Bonferroni tests for the one-way ANOVA test and the Dunn test for Kruskal Wallis analysis. Descriptive statistics of tissue TNF-α level and ZO-1, Occludin, and TLR-4 immunoreactivity density were expressed as med (min-max), and all remaining data were expressed as mean ± standard deviation. Data with $p < 0.05$ were considered statistically significant. As a consequence of the statistical analysis, the number of rats was calculated to be $n = 8$ with a 3% margin of error at the 0.05 significant level for the 80% power value. (Type I Error = 0.05, Power of Test = 0.80). Despite the risk of animal death, the LPS and LPS+MEL groups were calculated to have $n = 13$, 40% greater than the other groups.

Results

Body weight

The body weights of the rats were measured before and after the experiment. The comparison of the body weights were shown in Figure 1. The rats in the LPS group significantly lost weight at the end of the experiment ($p < 0.001$). At the end of the experiment, the weights of both the LPS+MEL group ($p < 0.05$) and MEL group ($p < 0.01$) had significantly higher than the LPS group.

Histopathological evaluation

The morphological and cellular changes in cerebral cortical brain tissues were examined by H&E

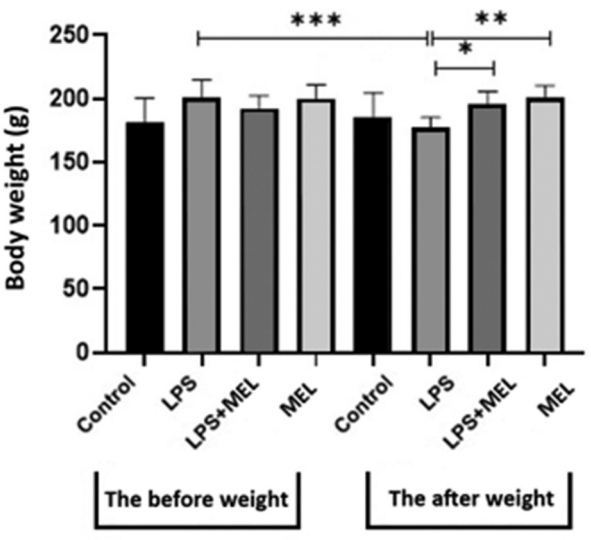

Figure 1. Comparison of body weights of rats belonging to all groups before and after the study. *$p < 0.05$, **$p < 0.01$, ***$p < 0.001$.

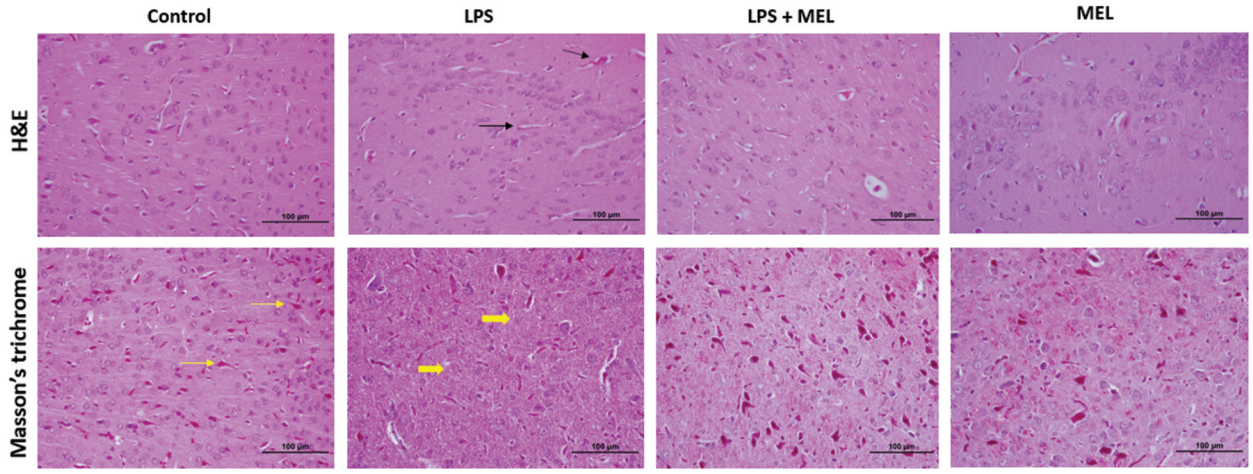

Figure 2. Light microscopic findings in the rat brain cortex (Olympus BX51, Tokyo, Japan. X40). Black arrow; vascular congestion, yellow arrow; eosinophilic stained neuron cell bodies, thick yellow arrow; pale stained necrotic neurons, red arrow; normal morphology neurons, thick red arrow; degenerative neurons with irregular pycnotic nuclei, thick black arrow; degenerative neurons with cytoplasmic vacuoles.

staining (Figure 2). No observable changes were founded in both control or MEL groups. However, impaired axons and vascular congestion were observed in the LPS group. Rare vascular congestion structures were observed in the LPS +MEL group compared to the LPS group. In addition, neuron structures and glial cells with similar characteristics to the control group were determined in the LPS+MEL group.

Masson's trichrome staining was also performed for visualization of connective tissue (Figure 2). The eosinophilic stained neuron cell bodies were observed in control brain tissue sections. Besides, necrotic neurons and vascular congestion were slightly observed in cortical areas of the LPS group.

Cresyl violet acetate staining was used to examine the nasal bodies of the surviving neurons in the brain cortex (Figure 3). In the control group, the number of viable neurons with distinct nuclear membranes was found to be higher than in the LPS group ($p < 0.001$). The degenerative neurons with irregular pycnotic nuclei and cytoplasmic vacuoles were observed in the cortical regions of the LPS group. The number of degenerative neurons both in the LPS+MEL group ($p < 0.01$) and in the MEL group ($p < 0.001$) was significantly reduced compared to the LPS group.

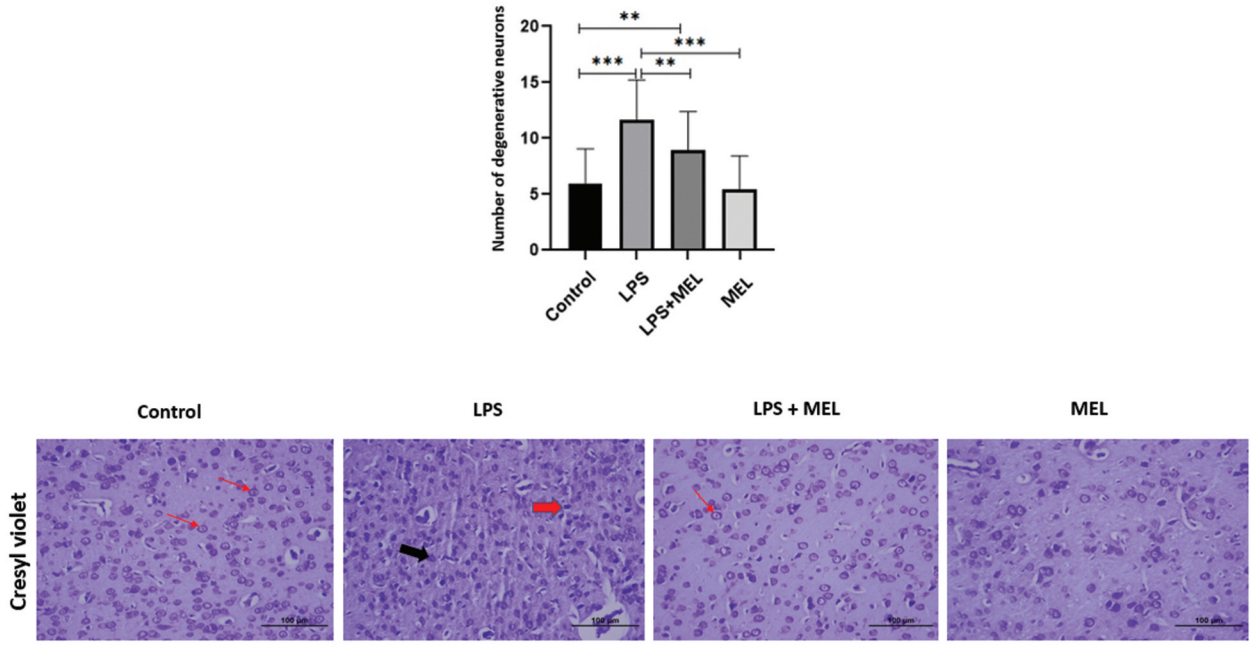

Figure 3. Light microscopic findings in the rat brain cortex (Olympus BX51, Tokyo, Japan. X40) and statistical analysis of degenerative neurons identified in the cerebral cortex area by Cresyl violet staining. *$p < 0.05$, **$p < 0.01$, ***$p < 0.001$. Red arrow; normal morphology neurons, thick red arrow; degenerative neurons with irregular pycnotic nuclei, thick black arrow; degenerative neurons with cytoplasmic vacuoles.

Immunoreactivity

The tight junction proteins of the blood-brain barrier such as ZO-1 and Occludin expressions and an inflammation marker TLR4 expression were visualized by immunohistochemical stainings (Figure 4a).

ZO-1 immunoreactivity density decreased significantly in the LPS group compared to the control group ($p < 0.001$) while ZO-1 expression in the MEL group increased significantly compared to the LPS group ($p < 0.05$). Also, ZO-1 expression in the LPS+MEL group decreased remarkably compared to the control group ($p < 0.05$) (Figure 4b and Table 1).

In addition, the Occludin immunoreactivity density of the LPS group decreased significantly compared to all other groups ($p < 0.001$ to control, $p < 0.001$ to MEL, $p < 0.001$ to LPS+MEL) (Figure 4b and Table 1).

Moreover, TLR-4 immunoreactivity density in the LPS group increased significantly compared to the control group ($p < 0.001$), and to the MEL group ($p < 0.001$), This density in the LPS+MEL group decreased statistically significantly compared to the LPS group ($p < 0.001$). MEL also decreased slightly TLR4 immunoreactivity compared to the LPS+MEL group ($p < 0.05$) (Figure 4b and Table 1).

Protein expression

ZO-1, Occludin, and TLR-4 protein expressions were further evaluated in brain tissue by western blotting.

It was determined that the expression of ZO-1 decreased in the LPS group compared to the control group ($p < 0.05$), and increased in the MEL group compared to the LPS group ($p < 0.05$). In addition, MEL treatment increased ZO-1 expression in the LPS+MEL group compared to the LPS group ($p > 0.05$) (Figure 5a and Table 2).

The expression of Occludin decreased in the LPS group compared to the control group. In addition,

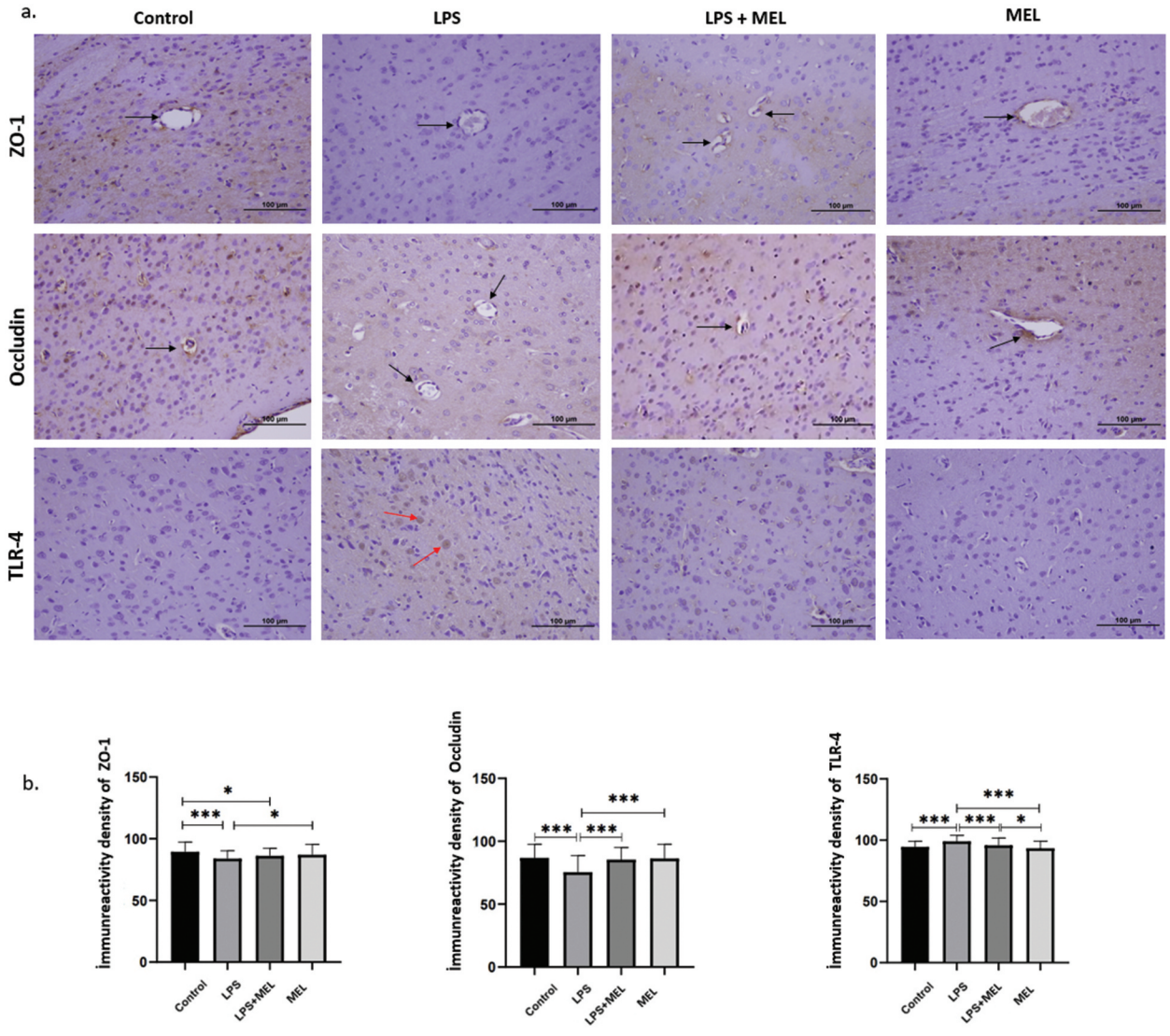

Figure 4. (a) immunohistochemical microscopic findings in the rat brain cortex (Olympus BX51, Tokyo, Japan. X40). ZO-1 and Occludin expression in cerebral cortex blood vessel endothelial cells (black arrow) and inflammation marker TLR-4 expression (red arrow). (b) Immunoreactivity density of ZO-1, Occludin, and TLR-4 in brain tissue. *$p < 0.05$, **$p < 0.01$, ***$p < 0.001$

Table 1. ZO-1, Occludin and TLR-4 immunoreactivity density of experimental groups. *$p < 0.05$, **$p < 0.01$, ***$p < 0.001$.

	Control ($n = 8$)	LPS ($n = 13$)	LPS + MEL ($n = 13$)	MEL ($n = 8$)
ZO-1	89,65 (85,01–93,64)	84 (79,05–89,15)	85,93 (80,42–92,24)	86,39 (82,92–89,68)
Occludin	87,15 (78,31–92,16)	74,15 (65,64–80,14)	85,23 (77,11–92,33)	85,23 (79,35–92,44)
TLR-4	95,46 (91,28–97,44)	98,55 (96,59–103,1)	94,46 (89,53–97,36)	97,08 (91,77–99,96)

ZO-1 İmmunreactivity density
***p < 0.001 Control and LPS group
*p < 0.05 Control and LPS+MEL group
*p<0.05 LPS and MEL group
Occludin İmmunreactivity density
***p < 0.001 Control and LPS group
***p < 0.001 LPS and LPS+MEL group
***p < 0.001 LPS and MEL group
TLR-4 İmmunreactivity density
***p < 0.001 Control and LPS group
***p < 0.001 LPS and LPS+MEL group
***p < 0.001 LPS and MEL group
*p < 0.05 LPS+MEL and MEL group

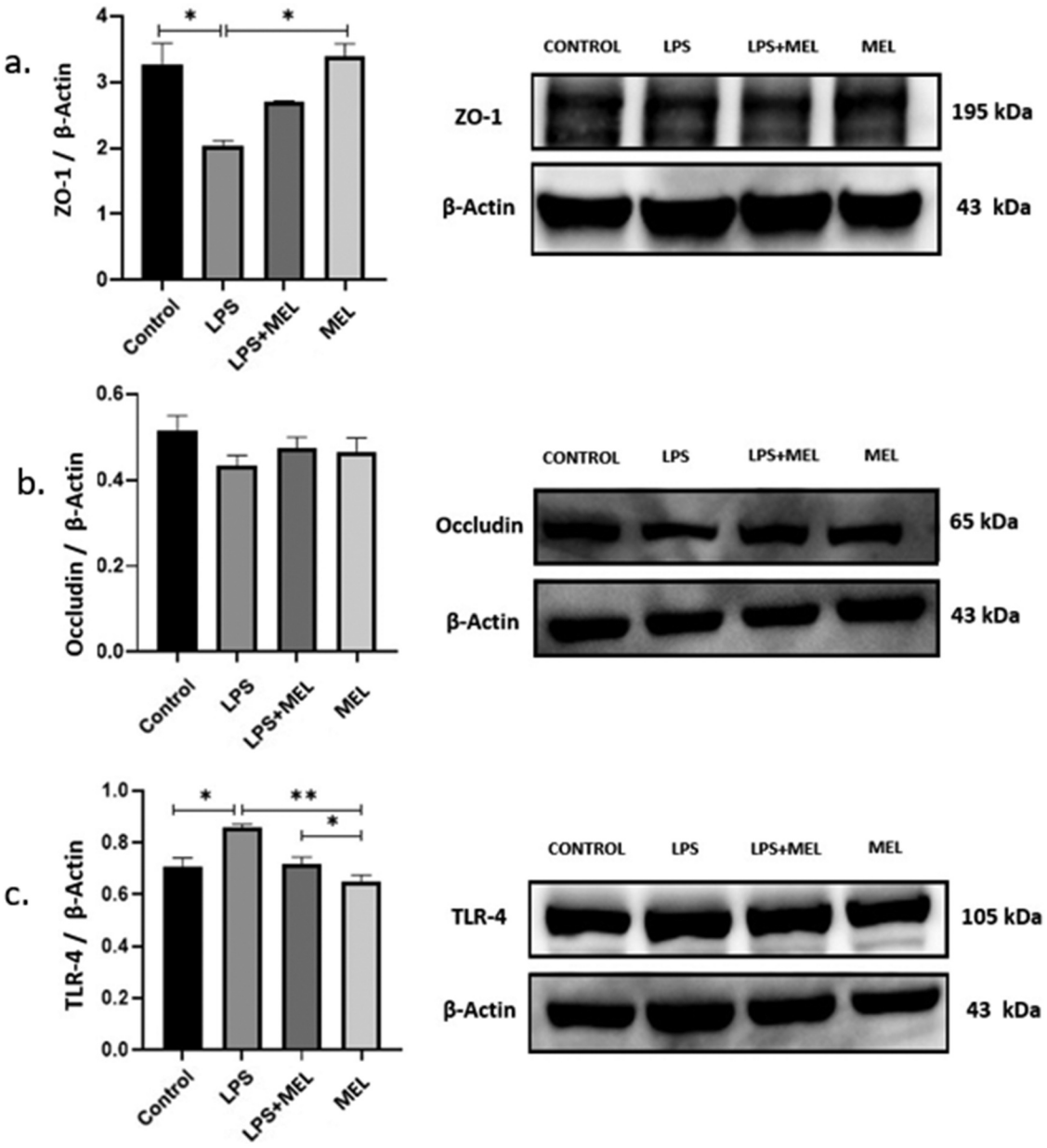

Figure 5. The brain tissue protein expression levels compared to β-actin protein bands were examined by Western blotting. (a) ZO-1. (b) Occludin. (c) TLR-4. *$p < 0.05$, **$p < 0.01$.

Table 2. ZO-1, Occludin and TLR-4 amount of protein of experimental groups. *$p < 0.05$, **$p < 0.01$, ***$p < 0.001$.

	Control ($n = 8$)	LPS ($n = 13$)	LPS + MEL ($n = 13$)	MEL ($n = 8$)
ZO-1	(3,276 ± 0,312)	(2,038 ± 0,078)	(2,710 ± 0,008)	(3,381 ± 0,203)
Occludin	(0,514 ± 0,035)	(0,432 ± 0,025)	(0,475 ± 0,024)	(0,466 ± 0,032)
TLR-4	(0,704 ± 0,036)	(0,858 ± 0,012)	(0,715 ± 0,028)	(0,647 ± 0,028)

ZO-1 amount of protein.
*$p < 0.05$ Control and LPS group.
*$p < 0.05$ LPS and MEL group.
TLR-4 amount of protein.
*$p < 0.05$ Control and LPS group.
**$p < 0.01$ LPS and MEL group.
*$p < 0.05$ LPS+MEL and MEL group.

Occludin expression of the LPS+ MEL group increased compared to the LPS group. These changes were not significant in terms of occludin expression ($p > 0.05$) (Figure 5b and Table 2).

The expression of TLR-4 as a marker of inflammation in tissue increased notably in the LPS group compared to the control group ($p < 0.05$). Besides, MEL treatment significantly reduced TLR4 expression compared to the LPS group ($p < 0.01$) and to the LPS +MEL group ($p < 0.05$) (Figure 5c and Table 2).

Lipid peroxidation level and antioxidant status

Tissue MDA, SOD, CAT, and GSH-Px levels were examined by the ELISA method in the damage caused by endotoxemia in the blood-brain barrier.

MDA is a product of lipid peroxidation. MDA brain tissue level in the LPS group increased significantly compared to the control group ($p < 0.001$). MEL treatment decreased MDA brain tissue level in the LPS +MEL group compared to the LPS group. However, this decrease was statistically not significant ($p > 0.05$). MEL treatment decreased significantly the MDA expression level in comparison to the LPS group ($p < 0.01$) (Figure 6a and Table 3).

SOD brain tissue level in the LPS group increased compared to the control group, but this increase was not statistically significant ($p > 0.05$) (Figure 6b and Table 3).

CAT brain tissue levels in LPS, LPS+MEL, and MEL groups were compared with the control group decreased. However, this decrease is statistically was not statistically significant ($p > 0.05$) (Figure 6c and Table 3).

GSH-Px brain tissue levels showed no statistically significant changes between the groups ($p > 0.05$) (Figure 6d and Table 3).

Inflammation

Tissue IL-1β, NF-kB, TGF-β, and TNF-α, levels were analyzed by ELISA method in the damage caused by LPS-induced endotoxemia in the blood-brain barrier.

IL-1β brain tissue level in the LPS group increased with a small difference compared to the control group ($p > 0.05$). In addition, the IL-1β brain tissue level in the LPS+ MEL group showed a statistically insignificant decrease compared to the LPS group ($p > 0.05$) (Figure 7a and Table 3).

NF-kB brain tissue level of the LPS group increased compared to all other groups. However, those changes were not statistically significant in terms of NF-kB brain tissue level ($p > 0.05$) (Figure 7b and Table 3).

When the TGF-β level in the brain tissue was considered, TGF-β brain tissue levels were not observed statistically changed in all groups ($p > 0.05$) (Figure 7c and Table 3).

There was a small increase in TNF-α brain tissue level in the LPS group compared to the control group. However, this increase was not statistically significant ($p > 0.05$) (Figure 7d and Table 3).

Discussion

This study investigated the histological and biochemical effects of melatonin against LPS-induced endotoxemia in rat brain tissue. Accordingly, it was shown that melatonin administration before LPS provided a significant reduction in severe BBB damage caused by LPS.

Endotoxemia, sepsis is a systemic inflammatory response syndrome with high morbidity and mortality rates worldwide. There has not been any effective cure for sepsis yet even though its known high risks. Organ damage caused by LPS-induced endotoxemia is mostly associated with the formation of reactive oxygen and nitrogen derivatives [1]. CNS is one of the most affected systems by oxidative stress in LPS-induced endotoxemia. The brain tissue is highly susceptible to oxidant stress due to excessive oxygen use, high metal content, and weak antioxidant defense mechanisms [5,6]. A systemic use of LPS alters the oxidative balance, and triggers the production of various free radicals, causing dysfunctions in CNS [25,26]. Meningitis, encephalitis, and local or systemic infections, especially sepsis, are known to alter the permeability of the BBB which is one of the protective barriers of CNS [27]. In a study, degenerative changes such as a dense and hyperchromatic nucleus in neurons, and irregularly shaped and wide perineuronal vacuolization

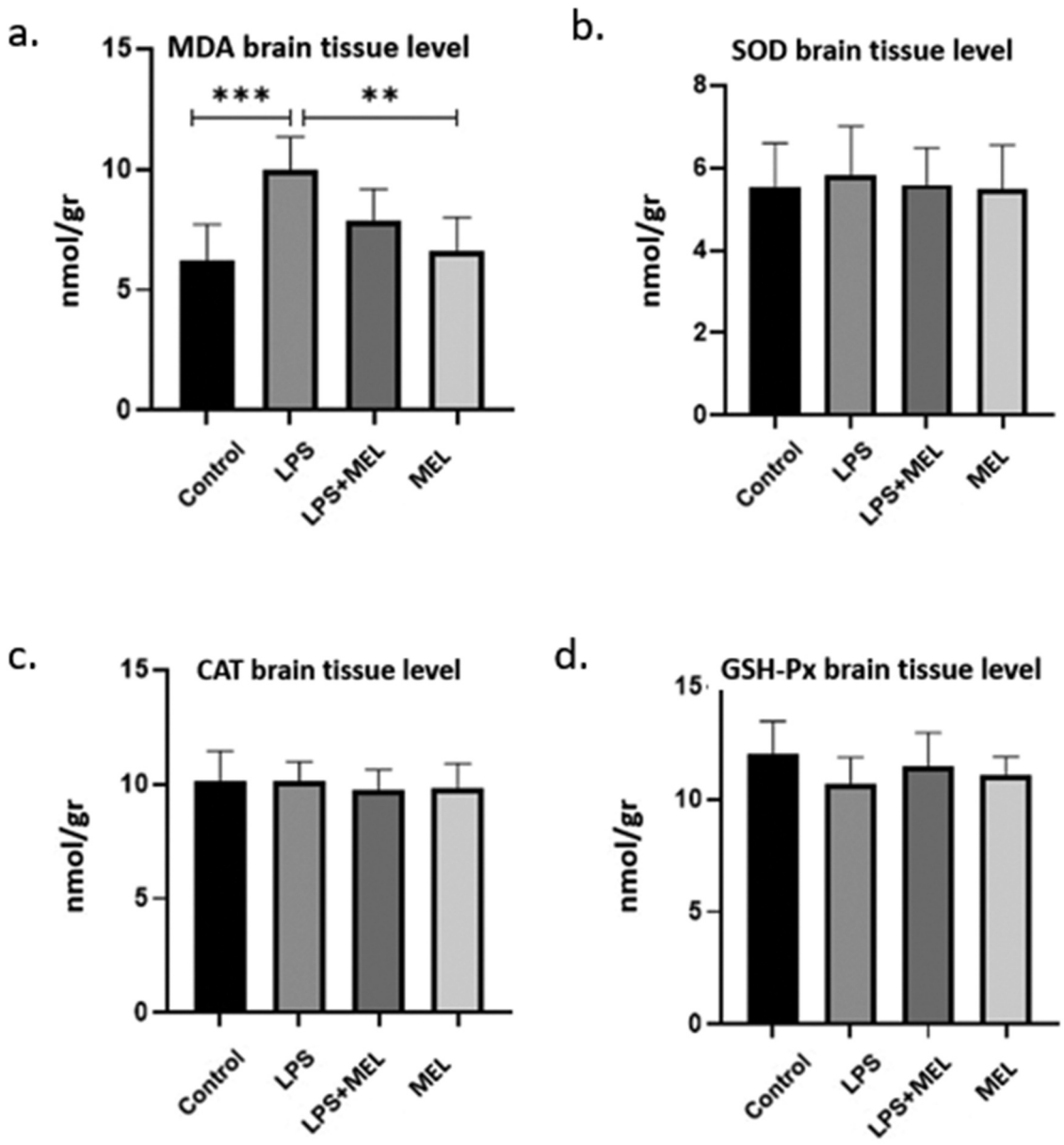

Figure 6. The brain tissue MDA, SOD, CAT, and GSH-Px levels were examined by ELISA method (a) MDA. (b) SOD. (c) CAT. (d) GSH-Px. $^{**}p < 0.01$, $^{***}p < 0.001$.

around degenerated neurons were observed in the cerebral cortex upon application of LPS [28]. In another sepsis model, neuron loss and neuronal pyknosis were detected in the LPS group [29]. In the acute neuroinflammation mouse model, astrocyte and endothelial cell loss, basal membrane destruction, and microhemorrhage were observed in astrocyte footprints edema of BBB. In the same study, a significant decrease in the expressions of occludin and ZO-1 was observed [30]. Consistent with our findings, occludin, and ZO-1 expression were substantially reduced in the LPS group in another rat experiment [31].

TLR-4 is one of the special receptors that recognize whole bacteria or bacterial products such as LPS and is an important research topic of endotoxemia experiments. Choi et al. conducted that TLR-4 is activated by LPS on human brain endothelial cell line [32]. In addition, it was reported that NF-κB and TLR-4 expression increased in the hippocampus in the LPS group of a neuroinflammation model in male Sprague-Dawley rats [33]. A further investigation discovered that TLR-4 levels boosted BV2 cell lines exposed to LPS-induced inflammation [34]. Our study's level of TLR-4 expression and the result of these investigations were correlated. The inflammatory mediators released from macrophages as a result of LPS induction damage in septic shock. These are inflammatory cytokines (IL-1, IL-6, IL-12, TNF-α), reactive oxygen and nitrogen metabolites, and arachidonic acid metabolites (prostaglandins, leukotrienes) [35]. Many scientific studies have reported that intraperitoneal LPS application increases the levels of many proinflammatory cytokines, especially IL-1β and TNF-α, in brain tissue [36–38]. Cytokine increase is

Table 3. MDA, SOD, CAT, GSH-Px, IL-1β, NF-κB, TGF-β, TNF-α ELISA brain tissue levels. *; $p < 0.05$, **; $p < 0.01$, ***; $p < 0.001$.

	Control ($n = 8$)	LPS ($n = 13$)	LPS + MEL ($n = 13$)	MEL ($n = 8$)
MDA	(6,176 ± 1,543)	(9,943 ± 1,403)	(7,873 ± 1,316)	(6,601 ± 1,413)
SOD	(5,526 ± 1,077)	(5,811 ± 1,200)	(5,593 ± 0,895)	(5,474 ± 1,074)
CAT	(10,150 ± 1,303)	(10,130 ± 0,857)	(9,746 ± 0,903)	(9,834 ± 1,070)
GSH-Px	(11,99 ± 1,487)	(10,710 ± 1,156)	(11,47 ± 1,485)	(11,060 ± 0,829)
IL-1β	(1735 ± 270,3)	(1783 ± 238,8)	(1757 ± 160,1)	(1686 ± 287,3)
NF-κB	(6,507 ± 0,873)	(6,929 ± 0,647)	(6,271 ± 0,514)	(6,474 ± 0,861)
TGF-β	(147,5 ± 19,21)	(181,1 ± 24,29)	(166,3 ± 24,81)	(169,2 ± 20,08)
TNF-α	85,57 (75,69–91,23)	90,09 (70,71–91,84)	82,16 (75,13–90,89)	82,94 (64,92–95,08)

MDA ELISA finding.
***$p < 0.001$ Control and LPS group.
**$p < 0.01$ LPS and MEL group.
TGF-β ELISA finding.
*$p < 0.05$ Control and LPS group.

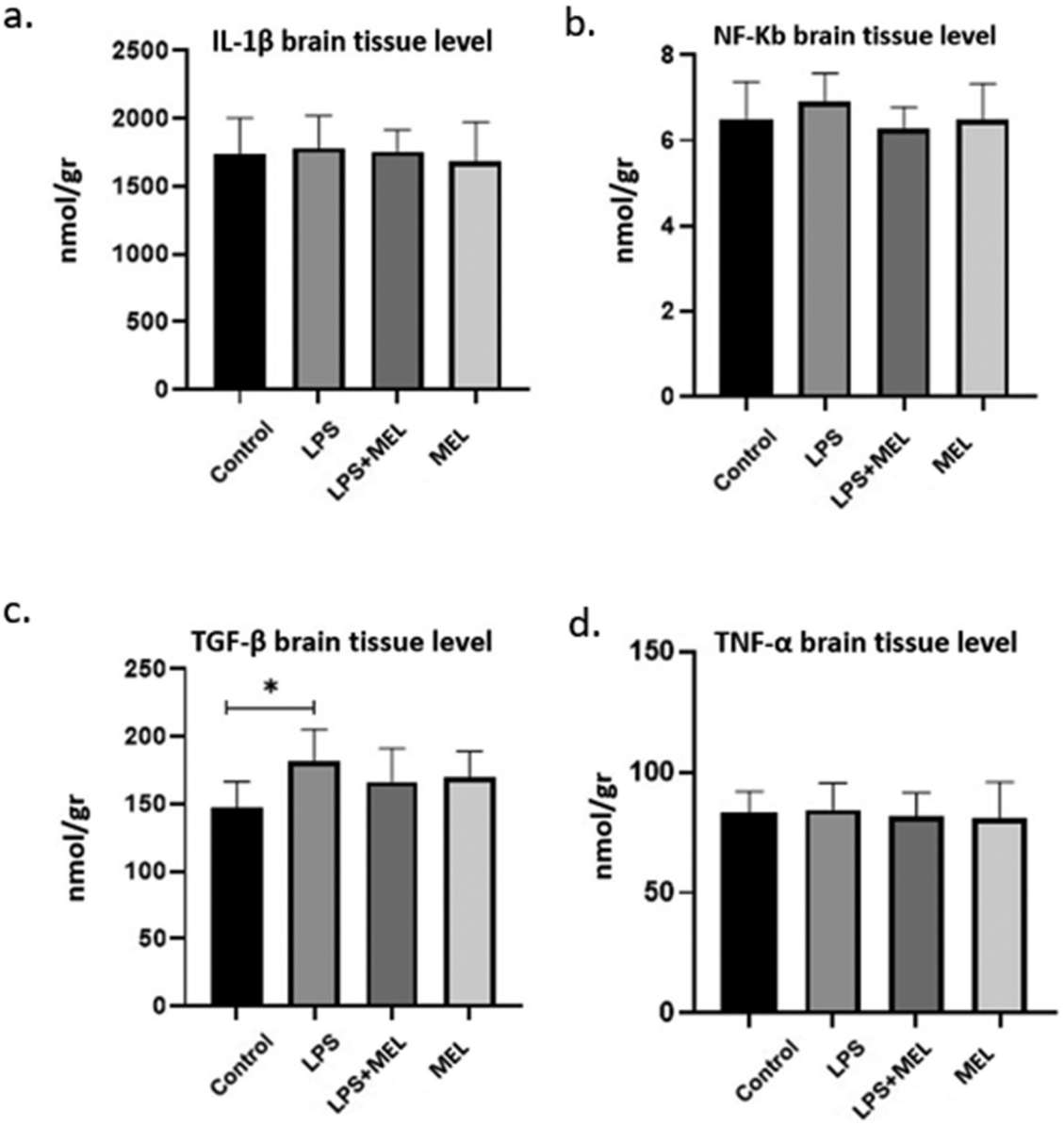

Figure 7. The brain tissue IL-1β, NF-κB, TGF-β, TNF-α levels examined by ELISA method. (a) IL-1β. (b) NF-κB. (c) TGF-β. (d) TNF-α.

stimulated by activating NF-kB primarily in the cascade of inflammation initiated by LPS through TLR-4. In addition, recent studies have revealed the positive roles of TGF-β in inflammatory responses. Important information is provided by measuring the levels of MDA, one of the oxidative stress markers brought on by inflammation in the brain. Along with MDA, SOD, CAT, and GSH-Px levels are some of the antioxidant enzymes that provide information about the oxidative stress level caused by inflammation. It was

found that the level of MDA increased in brain tissue in a study using LPS to produce an endotoxemia model, which is by the results of this study [39].

Melatonin (MEL), described as the 'night hormone', is an important free radical scavenger, antioxidant, and immunomodulator [40]. Melatonin has oncostatic, anti-inflammatory, and anticonvulsant effects, as well as critical physiological functions such as regulation of circadian rhythms and reproductive axis [41]. In a study, it was observed that MEL given before inflammation induced by LPS increased myelinization and recovered neuron morphology [42]. To our findings, different research found that melatonin given before LPS exposure reduced the neuronal damage caused by LPS [43]. Lee et al. observed that melatonin given at a dose of 10 mg/kg before the administration of 2 mg/kg LPS to pregnant mice improved BBB integrity [44]. Qin et al. evaluated BBB in the neuroinflammation model and stated that the expressions of occludin, claudin-5, and ZO-1 improved with MEL treatment [45]. MEL administered for protective purposes also improved the expression of ZO-1 and occludin in the brain. In addition, another study stated that melatonin suppresses the TLR-4/NF-kB signaling pathway [42]. Pretreatment with MEL alleviated LPS-induced TLR-4 expression in the brain. MEL is also known to stimulate many antioxidant enzyme activities such as GSH-Px, SOD, and CAT against oxidative stress [22]. Another study showed that treatment with MEL in formaldehyde-induced neurotoxicity reduced MDA levels while raising SOD ve GSH-Px levels [46]. Park et al. demonstrated that MEL reduced IL-1β and TNF-α levels in the LPS-induced inflammation model in BV-2 microglia cells [47]. It was shown that high levels of NF-kB binding activity were alleviated by MEL in the mouse meningitis model induced by LPS [48]. Contrary to our data, there is no study in the literature on the protective effect of melatonin on LPS neuroinflammation related to another marker TGF-β.

Conclusion

We investigated the BBB changes induced by endotoxemia in rats and the effects of MEL given in pharmacological doses on these changes in this study. MEL restored the BBB's impaired structure caused by endotoxemia, demonstrating its protection over tight junction proteins. MEL, an anti-inflammatory hormone, inhibited sepsis-induced brain inflammation, reducing the number of degenerative neurons.

Acknowledgments

This project was supported by the Scientific Research Unit of Bezmialem Vakıf University (BAP No: 11.2018/25).

Disclosure statement

No potential conflict of interest was reported by the authors.

Funding

The author(s) reported there is no funding associated with the work featured in this article.

ORCID

Kubra Tugce Kalkan http://orcid.org/0000-0001-7461-277X
Mukaddes Esrefoglu http://orcid.org/0000-0003-3380-1480
Sule Terzioglu-Usak http://orcid.org/0000-0002-4594-2697
Arzu Yay http://orcid.org/0000-0002-0541-8372

References

[1] Khodir AE, Ghoneim HA, Rahim MA, et al. Montelukast attenuates lipopolysaccharide-induced cardiac injury in rats. *Hum Exp Toxicol*. 2016;35(4):388–397. doi: 10.1177/0960327115591372
[2] Akira S, Takeda K. Toll-like receptor signaling. Nat Rev Immunol. 2004;4(7):499–511. doi: 10.1038/nri1391
[3] Xaio H, Banks WA, Niehoff ML, et al. Effect of LPS on the permeability of the blood–brain barrier to insulin. Brain Res. 2001;896(1–2):36–42. doi: 10.1016/S0006-8993(00)03247-9
[4] Pan W, Yu C, Hsuchou H, et al. Neuroinflammation facilitates LIF entry into the brain: role of TNF. Am J Physiol Cell Physiol. 2008;294(6):C1436–42. doi: 10.1152/ajpcell.00489.2007
[5] Facheris M, Beretta S, Ferrarese C, et al. Peripheral markers of oxidative stress and excitotoxicity in neurodegenerative disorders: tools for diagnosis and therapy? J Alzheimers Dis. 2004;6(2):177–184. doi: 10.3233/JAD-2004-6210
[6] Cemeli E, Smith IF, Peers C, et al. Oxygen-induced DNA damage in freshly isolated brain cells compared with cultured astrocytes in the comet assay. *Teratog Carcinog Mutagen*. 2003;23(S2):43–52. doi: 10.1002/tcm.10079
[7] Calabria AR, Shusta EV. Blood–brain barrier genomics and proteomics: elucidating phenotype, identifying disease targets and enabling brain drug delivery. Drug Discov Today. 2006;11(17–18):792–799. doi: 10.1016/j.drudis.2006.07.006
[8] Wolburg H, Noell S, Mack A, et al. Brain endothelial cells and the glia-vascular complex. Cell Tissue Res. 2009;335(1):75–96. doi: 10.1007/s00441-008-0658-9
[9] Deli MA, Abraham CS, Kataoka Y, et al. Permeability studies on in vitro blood–brain barrier models: physiology, pathology, and pharmacology. Cell Mol Neurobiol. 2005;25(1):59–127. doi: 10.1007/s10571-004-1377-8
[10] Banks WA, Robinson SM. Minimal penetration of lipopolysaccharide across the murine blood–brain barrier. Brain Behav Immun. 2010;24(1):102–109. doi: 10.1016/j.bbi.2009.09.001
[11] Wolburg H, Lippoldt A. Tight junctions of the blood–brain barrier: development, composition, and

regulation. Vasc Pharmacol. 2002;38(6):323–337. doi: 10.1016/S1537-1891(02)00200-8
[12] Mayhan WG, Heistad DD. Permeability of blood-brain barrier to various sized molecules. Am J Physiology. 1985;248(5):H712–8. doi: 10.1152/ajpheart.1985.248.5.H712
[13] Ziylan YZ, Robinson PJ, Rapoport SI. Blood-brain barrier permeability to sucrose and dextran after osmotic opening. Am J Physiol. 1984;247(4):R634–8. doi: 10.1152/ajpregu.1984.247.4.R634
[14] Rapoport SI. Pathological alterations of the blood-brain barrier. In: Blood-brain barrier in physiology and medicine. New York: Raven; 1976. pp. 129–152.
[15] Tucsek Z, Toth P, Sosnowska D, et al. Obesity in aging exacerbates blood-brain barrier disruption, neuroinflammation, and oxidative stress in the mouse hippocampus: effects on expression of genes involved in beta-amyloid generation and Alzheimer's disease. J Gerontol A Biol Sci Med Sci. 2014;69 (10):1212–1226. doi: 10.1093/gerona/glt177
[16] Sengillo JD, Winkler EA, Walker CT, et al. Deficiency in mural vascular cells coincides with blood–brain barrier disruption in a Alzheimer's disease. Brain Pathol. 2012;23(3):303–310. doi: 10.1111/bpa.12004
[17] Starr JM, Wardlaw J, Ferguson K, et al. Increased blood-brain barrier permeability in type II diabetes demonstrated by gadolinium magnetic resonance imaging. J Neurol Neurosurg Psychiatry. 2003;74 (1):70–76. doi: 10.1136/jnnp.74.1.70
[18] Abraham CS, Harada N, Deli MA, et al. Transient forebrain ischemia increases the blood-brain barrier permeability for albumin in stroke-prone spontaneously hypertensive rats. Cell Mol Neurobiol. 2003;22(4):455–462. doi: 10.1023/A:1021067822435
[19] Taguchi T, Testa JR, Mitcham JL, et al. Chromosomal localization of TIL, a gene encoding a protein related to the drosophila transmembrane receptor Toll, to human chromosome 4p14. Genomics. 1996;32 (3):486–488. doi: 10.1006/geno.1996.0150
[20] Medzhitov R, Janeway CA. Innate immunity: the virtues of a nonclonal system of recognition. Cell. 1997;91 (3):295–298. doi: 10.1016/S0092-8674(00)80412-2
[21] Mazgaeen L, Gurung P. Recent advances in lipopolysaccharide Recognition Systems. Int J Mol Sci. 2020;21(2):379. doi: 10.3390/ijms21020379
[22] Reiter RJ, Tan D, Terron MP, et al. Melatonin and its metabolites: new findings regarding their production and their radical scavenging actions. Acta Biochimica Polonica. 2007;54(1):1–9. doi: 10.18388/abp.2007_3264
[23] Şener G. Karanlığın hormonu: melatonin. Marmara Eczacılık Dergisi. 2010;3(14):112–120. doi: 10.12991/201014445
[24] Wang X. The antiapoptotic activity of melatonin in neurodegenerative diseases. CNS Neurosci Ther. 2009;15(4):345–357. doi: 10.1111/j.1755-5949.2009.00105.x
[25] Iraz M, Iraz M, Eşrefoğlu M, et al. Protective effect of β-glucan on acute lung injury induced by lipopolysaccharide in rats. *Turk J Med Sci*. 2015;45:261–267. doi: 10.3906/sag-1312-1
[26] Qin L, Wu X, Block ML, et al. Systemic LPS causes chronic neuroinflammation and progressive neurodegeneration. Glia. 2007;55(5):453–462. doi: 10.1002/glia.20467
[27] Nolan Y, Vereker E, Lynch AM, et al. Evidence that lipopolysaccharide-induced cell death is mediated by accumulation of reactive oxygen species and activation of p38 in rat cortex and hippocampus. Exp Neurol. 2003;184(2):794–804. doi: 10.1016/S0014-4886(03)00301-7
[28] Pollay M, Roberts PA. Blood-brain barrier: a definition of normal and altered function. Neurosurgery. 1980;6(6):675–685. doi: 10.1227/00006123-198006000-00014
[29] Ning Q, Liu Z, Wang X, et al. Neurodegenerative changes and neuroapoptosis induced by systemic lipopolysaccharide administration are reversed by dexmedetomidine treatment in mice. Neurological res. 2017;39 (4):357–366. doi: 10.1080/01616412.2017.1281197
[30] Deng S, Ai Y, Gong H, et al. Mitochondrial dynamics and protective effects of a mitochondrial division inhibitor, mdivi-1, in lipopolysaccharide-induced brain damage. Biochem Biophys Res Commun. 2018;496(3):865–871. doi: 10.1016/j.bbrc.2018.01.136
[31] Nicaise C, Mitrecic D, Demetter P, et al. Impaired blood–brain and blood–spinal cord barriers in mutant SOD1-linked ALS rat. Brain Res. 2009;1301:152–162. doi: 10.1016/j.brainres.2009.09.018
[32] Huang ZS, Da Qi X, Li Jun X, et al. Tetramethylpyrazine ameliorates lipopolysaccharide-induced sepsis in rats via protecting blood–brain barrier, impairing inflammation and nitrous oxide systems. Front Pharmacol. 2020;11:562084. doi: 10.3389/fphar.2020.562084
[33] Choi JJ, Choi YJ, Chen L, et al. Lipopolysaccharide potentiates polychlorinated biphenyl-induced disruption of the blood–brain barrier via TLR-4/IRF-3 signaling. Toxicology. 2012;302(2–3):212–220. doi: 10.1016/j.tox.2012.08.001
[34] Zhou J, Deng Y, Li F, et al. Icariside II attenuates lipopolysaccharide-induced neuroinflammation by inhibiting TLR-4/MyD88/NF-κB pathway in rats. Biomed Pharmacother. 2019;111:315–324. doi: 10.1016/j.biopha.2018.10.201
[35] Xu W, Luo T, Chai J, et al. Chlorogenic acid alleviates the inflammatory stress of LPS-induced BV2 cells via interacting with TLR4-mediated downstream pathways. Comput Math Methods Med. 2022;2022:1–6. doi: 10.1155/2022/6282167
[36] Diker S. İmmunoloji. Ankara: Medisan; 2005. p. 191–193.
[37] Turrin NP, Gayle D, Ilyin SE, et al. Pro-inflammatory and anti-inflammatory cytokine mRNA induction in the periphery and brain following intraperitoneal administration of bacterial lipopolysaccharide. Brain Res Bull. 2001;54(4):443–453. doi: 10.1016/S0361-9230(01)00445-2
[38] Quan N, Whiteside M, Herkenham M. Time course and localization patterns of interleukin-1β messenger RNA expression in brain and pituitary after peripheral administration of lipopolysaccharide. Neuroscience. 1998;83 (1):281–293. doi: 10.1016/S0306-4522(97)00350-3
[39] Gabellec MM, Griffais R, Fillion G, et al. Expression of interleukin 1α, interleukin 1β and interleukin 1 receptor antagonist mRNA in mouse brain: regulation by bacterial lipopolysaccharide (LPS) treatment. Mol Brain Res. 1995;31(1–2):122–130. doi: 10.1016/0169-328X(95)00042-Q
[40] Abdel Salam OM, Youness ER, Mohammed NA, et al. Effect of propofol and fentanyl on brain oxidative stress after systemic lipopolysaccharide injection in rats. React Oxyg Species (Apex). 2021;11:1–13. doi: 10.20455/ros.2021.r.801

[41] Pandi-Perumal SR, Trakht I, Srinivasan V, et al. Physiological effects of melatonin: role of melatonin receptors and signal transduction pathways. Prog Neurobiol. 2008;85(3):335–353. doi: 10.1016/j.pneurobio.2008.04.001

[42] Macchi MM, Bruce JN. Human pineal physiology and functional significance of melatonin. Front Neuroendocrinol. 2004;25(3–4):177–195. doi: 10.1016/j.yfrne.2004.08.001

[43] Hu Y, Wang Z, Pan S, et al. Melatonin protects against blood-brain barrier damage by inhibiting the TLR-4/NF-κB signaling pathway after LPS treatment in neonatal rats. Oncotarget. 2017;8(19):31638. doi: 10.18632/oncotarget.15780

[44] Favrais G, Saliba E, Savary L, et al. Partial protective effects of melatonin on developing brain in a rat model of chorioamnionitis. Sci Rep. 2021;11(1):1–12. doi: 10.1038/s41598-021-01746-w

[45] Lee JY, Song H, Dash O, et al. Administration of melatonin for prevention of preterm birth and fetal brain injury associated with premature birth in a mouse model. Am J Reprod Immunol. 2019;82(3):e13151. doi: 10.1111/aji.13151

[46] Qin W, Li J, Zhu R, et al. Melatonin protects blood-brain barrier integrity and permeability by inhibiting matrix metalloproteinase-9 via the NOTCH3/NF-κB pathway. Aging. 2019;11(23):11391. doi: 10.18632/aging.102537

[47] İlter K, Zararsiz G, Ögetürk M, et al. Formaldehit Nörotoksisitesine Bağlı Hipokampusta Gelişen Oksidatif Hasar ve Melatonin Hormonunun Koruyucu Etkisi: Deneysel Bir Çalışma. Fırat Tıp Dergisi. 2007;12(4):256–260.

[48] Park E, Chun HS. Melatonin attenuates manganese and lipopolysaccharide-induced inflammatory activation of BV2 microglia. *Neurochem Res*. 2017;42(2):656–666. doi: 10.1007/s11064-016-2122-7